Homodyne reflectometer for neutral beam injection interlock on large helical device

Homodyne reflectometer for neutral beam injection interlock on large helical device

K. Tanaka,[a] A. Ejiri,[b] Y. Ito, K. Kawahata, T. Tokuzawa, M. Osakabe, and Y. Takeiri
National Institute for Fusion Science, Toki 509-5292, Japan

(Received 7 May 2006; presented on 9 May 2006; accepted 7 June 2006; published online 3 October 2006)

Neutral beam injection (NBI) into low-density plasmas can cause serious damage to the vacuum vessel wall. It is necessary to stop the NBI when the plasma terminates. This needs a reliable density monitor for NBI interlock. A three-channel homodyne reflectometer, installed on a large helical device was used for an NBI interlock. Microwaves of 28.5, 34.9, and 40.2 GHz were injected with O mode polarization. At present, a simple homodyne detection scheme is used. The reflected signal consists of a dc component due to local and reflected power and an ac component due to fluctuations in the position of the cutoff layer. Since the change in dc signal was very small, the root mean square value of the ac signal was used as the interlock signal. At present the 34.9 GHz O mode channel, whose O mode cutoff density is 1.5×10^{19} m^{-3}, is used for the interlock. The system has been working since the first NBI experiments on LHD in 1999. © *2006 American Institute of Physics.* [DOI: 10.1063/1.2222169]

I. INTRODUCTION

A reliable neutral beam injection (NBI) interlock system is required in magnetically confined plasma devices such as tokamaks, stellarators, and helical devices. In a large helical device (LHD), the armor tiles at the NBI dump are designed to endure 100 ms exposure at full NBI power (7.5 MW) with no target plasma. Though there is no magnetic disruption on LHD, the plasma can terminate unexpectedly due to radiation collapse. If the NBI continues after plasma termination, the full neutral beam power is deposited on the vessel wall which can cause serious damage. The NBI shine-through ratio is more than 50% at densities lower than 1×10^{19} m^{-3}.[1] Therefore, the NBI has to be stopped when the density decreases below this value.

There are several possible diagnostics for the interlock source. First we consider an interferometer. Though this is the most accurate density monitor, fringe jump errors can occur at high density, so it is not reliable enough. The second possibility is a polarimeter. Recently, a polarimeter was used for density measurements in a well known magnetic field.[2,3] This is reasonably accurate and reliable; however, because the phase shift due to either Faraday rotation or the Cotton-Mutton effect is small, it is technically difficult as a routine diagnostic. The third possibility is plasma spectral emission measurements (e.g., Hα). This is simple, but the intensity is a function not only of density but also of temperature and neutral density, so it is not accurate. Finally, we propose a microwave reflectometer. It is expected to be a simple and reliable density monitor.

[a]Author to whom correspondence should be addressed; electronic mail: ktanaka@nifs.ac.jp
[b]Also at the Graduate School of Frontier Sciences, University of Tokyo, Kashiwa 277-8561, Japan.

II. SYSTEM SETUP

Figure 1 shows a schematic diagram of transmission and detection components of the density interlock reflectometer. The system has three channels with frequencies at 28.5, 34.9, and 40.2 GHz, which correspond to O mode cutoff densities of 1, 1.5, and 2×10^{19} m^{-3}, respectively. The transmission and detection components are located 8 m away from the port to reduce the influence of the magnetic field on microwave components.

The measurement scheme is a simple homodyne method, where the obtained signals are described as follows:

$$I_{\mathrm{homo}} \propto P_R + P_L + 2\sqrt{P_R P_L}\cos(\phi_0 + \phi_n), \quad (1)$$

where P_R is the reflected power, P_L the local power, ϕ_0 the phase shift due to cutoff position, and ϕ_n the phase shift due to fluctuation.

The first and second terms are dc components and the third term has an ac component. The reflected dc power (P_R) is much smaller than the local dc power (P_L). So, it is difficult to judge whether or not density reached the cutoff density. Therefore, fluctuation signal, which is the third term of Eq. (1), was used as a source of interlock.

Figure 2 shows a cross section of the microwave injection system. The polarization is O mode near the last closed

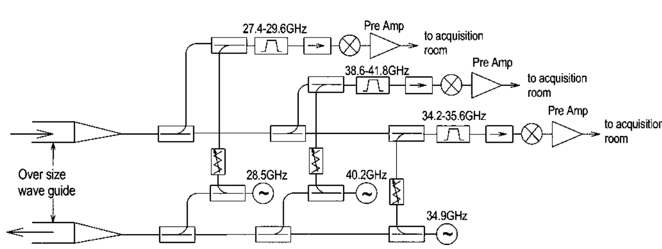

FIG. 1. Schematic diagram of transmission and detection components of a three-channel homodyne interlock reflectometer.

0034-6748/2006/77(10)/10E912/3/$23.00

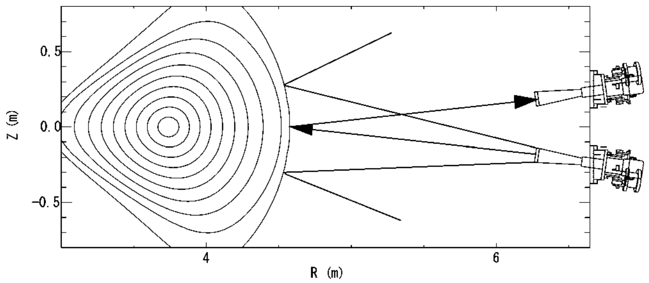

FIG. 2. Cross section of injection. Flux surfaces are shown from ρ (normalized radial position)$=0.1-1.0$ every $\rho=0.1$ step.

flux surface to be most sensitive to the density at the plasma boundary. The injected and detected beams lie in a plane tilted 45° between the major radial and toroidal directions. This plane was selected because it had a flat cutoff layer in order to receive reflected wave effectively. The $1/e^2$ intensity beamwidth is 550 mm for 28.5 and 34.9 GHz and 400 mm for 40.2 GHz. Because of the large beam size, the antenna alignment is insensitive to the signal intensity.

Figure 3 shows a schematic diagram of signal processing. The ac components of reflected signals are transmitted to the acquisition room via shielded co-axial cable. The signals are then bandpass filtered between 10 and 500 kHz and are rectified and filtered in order to convert to a root mean square (rms) signal. Finally, the rms signals are transmitted to the NBI control room by optical fiber where the interlock threshold level is set.

III. EXAMPLES OF OPERATION

In typical NBI discharges in LHD, 82.6 or 168 GHz electron cyclotron resonance heating initially produces the plasma, which is then heated by NBI. Since the density of ECRH plasmas sometimes does not exceed 1×10^{19} m^{-3}, the interlock system is overridden for a dead time of about 100 ms after the start of NBI. This dead time is varied depending on plasma operation. Usually, after NBI starts, the density quickly exceeds 1×10^{19} m^{-3}; therefore, wall damage due to the operation of NBI during the interlock dead time is not a problem.

Figure 4 shows an example of a discharge, in which the reflectometer interlock activated. A signal of 34.9 GHz was used as an interlock source because its signal intensity was strongest. A radiation-induced collapse occurred very quickly. In this discharge, the NBI pulse was programmed to occur during $t=0.4-9.4$ s, but the plasma suddenly terminated at $t=4.1$ s because of the radiation collapse. Between $t=0.9$ s and $t=3.78$ s, the line average density increased gradually at almost constant radiation power. At $t=3.6$ s, the

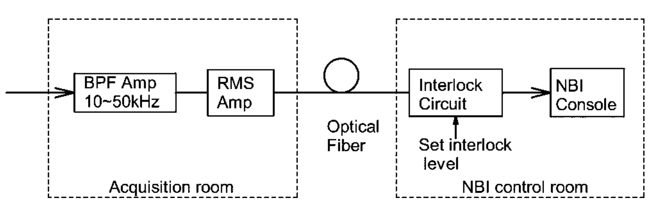

FIG. 3. Schematic diagram of the signal processing of the interlock system.

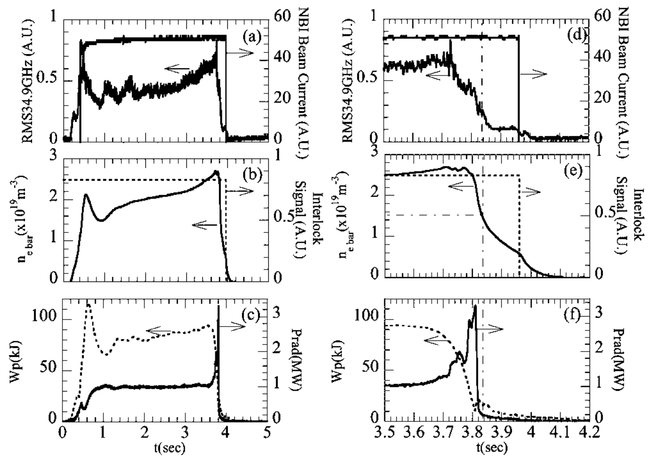

FIG. 4. Example of quick collapse. Time trace of [(a) and (c)] 34.9 GHz rms signal and NBI beam current, [(b) and (e)] line averaged density and interlock signal, and [(c) and (f)] stored energy and radiation power. Thin vertical dotted lines in [(d)–(f)] indicate the timing when the averaged density reaches 1.5×10^{19} m^{-3}, which is a 34.9 GHz O mode cutoff density.

radiation power started to increase and the diamagnetic stored energy started to decrease. This was because the injected NBI power was not high enough after $t=3.6$ s for the given plasma density. At $t=3.78$ s, the average density started to decrease. As shown in Figs. 4(d) and 4(e), the rms value of the 34.9 GHz reflected signal and the line average density follow almost the same trace. As shown in Fig. 4(d), the rms value of the 34.9 GHz reflected signal was nonzero after $t=3.83$ s, when the density became lower than the 34.9 GHz cutoff density (1.5×10^{19} m^{-3}). The nonzero signal during this time period might be due to forward scattering.

Figure 5 shows the relationship between the line average density and the rms value of the 34.9 GHz reflected signal of the discharge in Fig. 4. The different symbols are used to distinguish the data before and after radiation collapse. Generally, the 34.9 GHz rms signal was proportional to density in this discharge; however, the trace during the density increase phase was not identical to that after radiation collapse. The interlock level was set at 0.1 A.U. of the 34.9 GHz rms

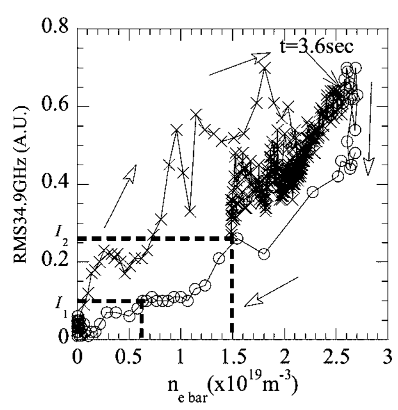

FIG. 5. Relation between the line averaged density and the 34.9 GHz rms signal of Fig. 4. I_1 and I_2 indicate the set interlock level and the rms signal corresponding cutoff density, respectively. The cross and circular symbols indicate the data before and after $t=3.6$ s, respectively.

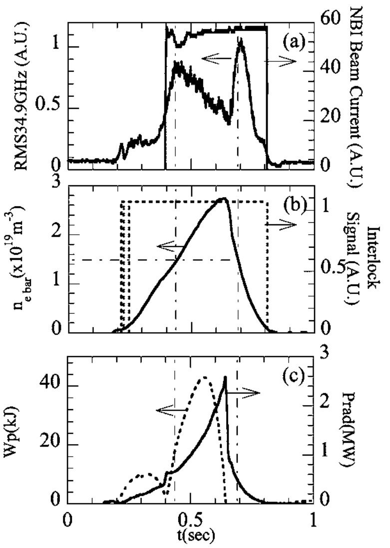

FIG. 6. Example of slow collapse. Time trace of (a) 34.9 GHz rms signal and NBI beam current, (b) line averaged density and interlock signal, and (c) stored energy and radiation power. Thin vertical dotted lines indicate the timing when the averaged density reaches 1.5×10^{19} m^{-3}, which is a 34.9 GHz O mode cutoff density.

signal. This corresponds to 0.6×10^{19} m^{-3}, which is lower than the 34.9 GHz O mode cutoff density $(1.5\times10^{19}$ m$^{-3})$.

Figure 6 shows another example, in which the interlock system worked. The radiation collapse occurred slowly. The radiation started to increase from the beginning of the discharge. This was probably due to the bad wall conditioning. The impurities penetrated into the plasma and enhanced radiation power. Unlike in Fig. 4, the time trace of the 34.9 GHz rms signal is very different from the line average density time trace. The 34.9 GHz rms signal increased until $t=0.44$ s, when the average density reach the 34.9 GHz O mode cutoff density $(1.5\times10^{19}$ m$^{-3})$. However, the 34.9 GHz rms signal started to decrease after this timing. Unlike in Fig. 4, the 34.9 GHz rms signal did not follow the time trace of average density. The discharge in Fig. 6 was not stable, so plasma parameter profiles such as density and temperature changed temporally throughout the discharge. This might cause a complicated signal behavior.

Figure 7 shows the relation between the line average density and the rms value of the 34.9 GHz reflected signal of the discharge in Fig. 6. The different symbols are used to distinguish the data between the density-increasing and density-decreasing phases. When the density is higher than 1.2×10^{19} m^{-3}, the rms signal is inversely proportional to the average density. The interlock level was set at 0.1 A.U., which was the same setting of discharge in Fig. 4; then the interlock system worked when density decreased to 0.1×10^{19} m^{-3}. Although the interlock level was the same setting of discharges in Figs. 4 and 5, the interlock activated at different densities.

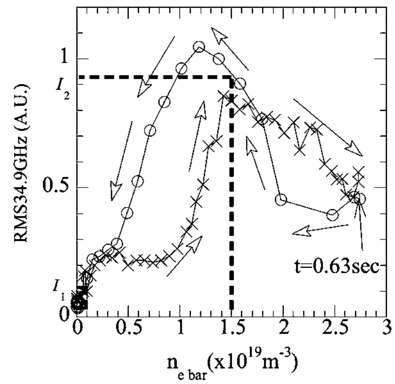

FIG. 7. Relation between the line averaged density and the 34.9 GHz rms signal of Fig. 6. I_1 and I_2 indicate the set interlock level and the rms signal corresponding cutoff density, respectively. The cross and circular symbols indicate the data before and after $t=0.63$ s, respectively.

The homodyne reflected signal is not a simple function of density and does not change in a steplike manner when the density exceeds the cutoff density. In particular, in a slow radiation collapse case like that in Fig. 5, the behavior of the rms signal is complicated. The corresponding signal level to the 34.9 GHz O mode cutoff density is 0.93 A..U. If the interlock level was set to be at 0.93 A.U., the interlock would not activate at higher than 1.5×10^{19} m^{-3} because the rms signal was smaller than 0.93 A.U. and the average density is higher than 1.5×10^{19} m^{-3} at $t=0.44-0.69$ s.

The interlock should work to protect the vacuum vessel. On the other hand, if interlock works too much, experiments are disturbed. Presently, the interlock level is determined empirically, and the lower interlock level corresponding to the lower interlock density is used. There is a risk to the damage vessel wall although experiments are not disturbed by the too frequent interlock. The damage of the vessel wall is also monitored by the infrared camera[4] to support the interlock system to check the heat load of the vessel wall.

[1] S. Murakami, N. Nakajima, and M. Okamoto, Trans. Fusion Technol. **27**, 256 (1995).
[2] Y. Kawano, S. Chiba, and A. Inoue, Rev. Sci. Instrum. **72**, 1068 (2001).
[3] T. Akiyama *et al.*, Rev. Sci. Instrum., these proceedings.
[4] M. Osakabe *et al.*, Rev. Sci. Instrum. **72**, 590 (2001).